

Article

A Power Prediction Method for Photovoltaic Power Plant Based on Wavelet Decomposition and Artificial Neural Networks

Honglu Zhu ¹, Xu Li ^{1,*}, Qiao Sun ², Ling Nie ², Jianxi Yao ¹ and Gang Zhao ³

Received: 13 October 2015; Accepted: 15 December 2015; Published: 24 December 2015

Academic Editor: Tapas Mallick

¹ School of Renewable Energy, North China Electric Power University, Beijing 102206, China; hongluzhu@126.com (H.Z.); jianxiyao@ncepu.edu.cn (J.Y.)

² Beijing Guodiantong Network Technology Co., Ltd., Beijing 100070, China; sunqiao@sgepri.sgcc.com.cn (Q.S.); nieling@sgepri.sgcc.com.cn (L.N.)

³ School of Electronic Engineering, Xidian University, Xian 710071, China; gangzhao@mail.xidian.edu.cn

* Correspondence: lixu_ncepu@126.com; Tel.: +86-153-3023-5680; Fax: +86-10-6177-1816

Abstract: The power prediction for photovoltaic (PV) power plants has significant importance for their grid connection. Due to PV power's periodicity and non-stationary characteristics, traditional power prediction methods based on linear or time series models are no longer applicable. This paper presents a method combining the advantages of the wavelet decomposition (WD) and artificial neural network (ANN) to solve this problem. With the ability of ANN to address nonlinear relationships, theoretical solar irradiance and meteorological variables are chosen as the input of the hybrid model based on WD and ANN. The output power of the PV plant is decomposed using WD to separated useful information from disturbances. The ANNs are used to build the models of the decomposed PV output power. Finally, the outputs of the ANN models are reconstructed into the forecasted PV plant power. The presented method is compared with the traditional forecasting method based on ANN. The results shows that the method described in this paper needs less calculation time and has better forecasting precision.

Keywords: photovoltaic power prediction; wavelet decomposition; artificial neural network; theoretical solar irradiance; signal reconstruction

1. Introduction

As energy supply and the environmental situation becomes increasingly tight and critical around the world, the contradiction between electricity power supply and demand stands out. The development and utilization of conventional energy sources suffer from increasing limitations. Solar energy is recognized as an ideal renewable energy power generation source. PV power generation is an important solar energy utilization pattern, but the output of PV power plants is highly random, with a fluctuating and intermittent nature. The grid-connection of large-scale PV power generation will bring about severe challenges to the safe and stable operation of grid and guaranteed electric power quality. Forecasting the output power of PV plant is a significant problem for electric power departments to adjust dispatch planning in time, boost the reliability of electric system operation and the connection level of PV power plants and reduce spinning the reserve capacity of generation systems [1,2].

In the past few years, PV power forecasting has been widely studied. Short-term power prediction methods for PV power plants mainly include two categories: physical methods and statistical methods. Physical methods mean that a physical equation is established for forecasting according to the PV power

generation process and system characteristics and in combination with forecast weather data [3,4]. Statistical methods aim to summarize inherent laws to forecast the output power of PV power plants based on historical power data [1,2,5–9]. The above methods have their respective advantages, but the non-stationary characteristics of PV power output has an important influence on the convergence and properties of the above methods.

Since solar irradiance received at a site on the Earth's surface shows periodicity and non-stationary characteristics due to the influence of Earth's rotation and revolution, output power data of PV plants shows one day periodicity. In other words, the power output presents a rising trend before noon, and presents a declining trend after noon. If an effective method to reduce the non-stationary characteristics of PV output power is not adopted, conventional power prediction methods cannot guarantee the precision of forecasting results, or even the convergence of the method [10]. Wavelet analysis methods can effectively extract the nonlinear and non-stationary features from original signals [1,5,11]. They are applicable to analyzing the fluctuations of renewable energy sources with obvious intermittent and non-stationary characteristics. Relevant research has achieved good results in wind power prediction [12].

Thus, in order to deal with the periodic and non-stationary problems of PV output power, a hybrid modeling method based on WD and ANN is proposed in the paper, to achieve both good algorithm convergence and prediction results. This paper is organized as follows: Section 2 analyzes the periodicity and non-stationary characteristics of PV output. Section 3 describes the PV power output decomposition process. Section 4 demonstrates the hybrid prediction method which combines wavelet decomposition and neural networks. Section 5 verifies and compares the effectiveness of the proposed method. Section 6 offers the conclusions of this study.

2. Analysis of Photovoltaic (PV) Output Characteristics

2.1. Periodicity and Non-Stationary Characteristics of Photovoltaic (PV) Output

The data used in the paper are from the PV testing platform of the State Key Laboratory of Alternate Electrical Power System with Renewable Energy Sources at North China Electric Power University in Changping District (Beijing, China), recorded with a sampling interval of 1 min. Table 1 shows the detailed information of the PV testing platform.

Table 1. PV power plant information.

Item	Data	Item	Data
Longitude	116.3059°E	Mounting disposition	Flat roof
Latitude	40.08914°N	Field type	fixed tilted plane
Altitude	80m	Installed capacity	10 kWp
Azimuth	0°	Technology	polycrystalline silicon
Tilt	37°	PV module	JKM245P

Figure 1 shows the output of the PV power plant for 5 days. It is known from the figure that the power output curve is influenced by the Earth's rotation with a period of one day, the output is 0 during the non-illuminated time at night and rises in the forenoon, and then declines in the afternoon. Influenced by the surrounding meteorological factors, the output power of the PV power plant shows different characteristics every day. The output characteristics of the PV power plant under different weather conditions are analyzed. Figure 2 shows the output curves of the PV power plant under four typical weather conditions: clear day, cloudy day, overcast day and rainy day. The solid line is the measured output of the PV power plant, while the dotted line is the theoretical output of the PV power plant, while the four colors correspond to the four seasons. Figure 2a, corresponding to a clear day, shows the measured output of the PV power plant is similar to the theoretical output; In Figure 2b, on a cloudy day, the measured output curve of the PV power plant fluctuates frequently

due to the movement of clouds in the sky; In Figure 2c, on an overcast day, the measured PV power plant output declines significantly, and the fluctuation is smaller than in cloudy weather; In Figure 2d, on a rainy day, the measured output of the PV power plant may show a huge decline. Influenced by seasonal factors, the global solar irradiance curve has obvious amount differences. It is highest in summer, followed by spring, autumn and winter. In brief, the daily output power of the PV power plant shows nonlinear characteristics from day to night; while the output of the PV power plant has obvious differences in the total amount during different seasons in a 1-year period. It can be seen that conventional power prediction methods based on time series are not applicable to the output power of a PV power plant.

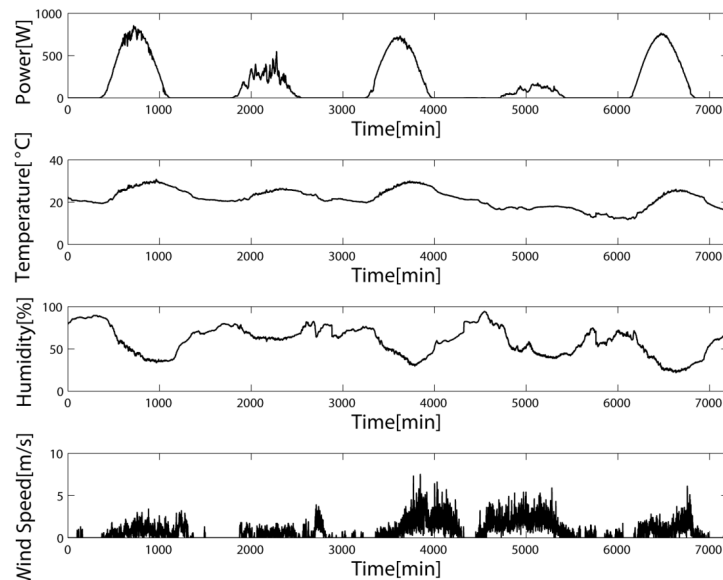


Figure 1. Output and meteorological factors of a PV power plant.

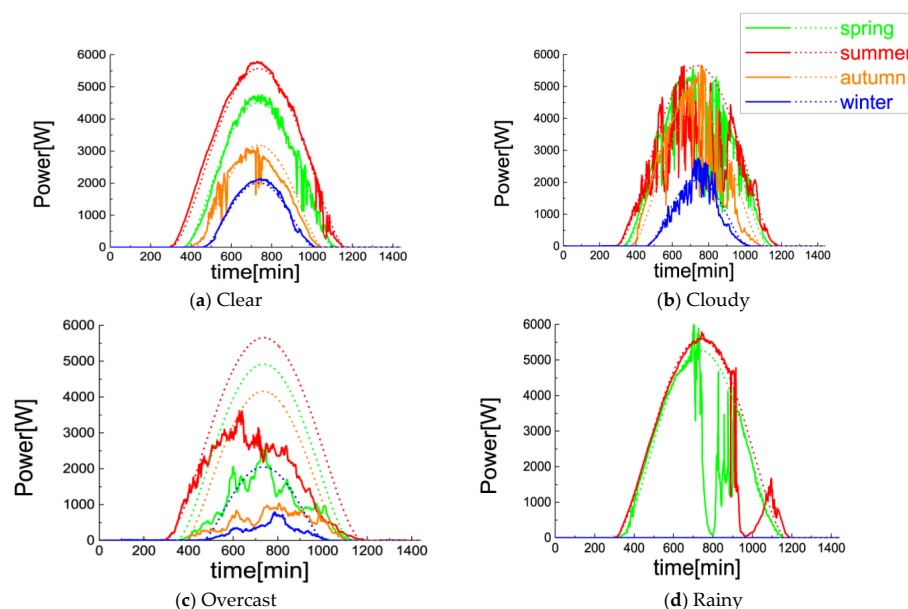


Figure 2. Output of a PV power plant during typical seasons and under typical weather conditions. (a) Daily PV output on clear day during typical seasons, (b) Daily PV output on cloudy day during typical seasons, (c) Daily PV output on overcast day during typical seasons, (d) Daily PV output on rainy day during typical seasons.

2.2. Influence of Meteorological Factors on Photovoltaic (PV) Output and Model Input Selection

To establish an accurate and reliable output power prediction model for a PV power plant, it is necessary to analyze the effect factors for the PV power plant output. In the physical sense, global solar irradiance received on the ground is a direct influencing factor on the voltage effect of PV cells. Meanwhile, PV output is also influenced by various kinds of meteorological conditions (Figure 1). Table 1 illustrates the correlation of output power with irradiance, temperature and humidity for each typical weather condition. The Pearson product-moment correlation coefficient, also known as r , can measure the direction and strength of the linear relationship between two variables, which is a method to quantify non-deterministic relationship. We use r to select the inputs for the forecasting model. The term r can be defined as follows:

$$r = \frac{\sum_{i=1}^N (X(i) - \bar{X}) \times (Y(i) - \bar{Y})}{\sqrt{\sum_{i=1}^N (X(i) - \bar{X})^2} \times \sqrt{\sum_{i=1}^N (Y(i) - \bar{Y})^2}} \quad (1)$$

where, N is the length of time series; i is the series number; X is the output power of the PV power plant; Y is one of the meteorological conditions, namely irradiance, temperature, humidity or wind speed.

It can be seen from Table 2 that the correlation coefficient between the power output of a PV power generator and solar irradiance is greater than 0.8, which means they are highly correlated, while the correlation coefficient between PV power generation output and temperature is greater than 0.3, which means these factors are positively and low-level correlated. The correlation coefficient of humidity indicates a low but negative correlation. The correlation between PV power generation output and wind speed is small.

Table 2. Pearson product-moment correlation coefficient between PV output and environmental factors under typical weather conditions.

Weather Condition	Pearson Product-Moment Correlation Coefficient			
	Irradiance	Temperature	Humidity	Wind Speed
Clear	0.966	0.322	-0.527	-0.229
Cloudy	0.891	0.441	-0.511	-0.025
Overcast	0.987	0.409	-0.478	0.125
Rainy	0.923	0.410	0.039	-0.178

3. Wavelet Decomposition (WD) for Photovoltaic (PV) Power Output

3.1. Wavelet Decomposition (WD) Fundamentals

The wavelet transform method [1,13] is a mathematical tool, much like a Fourier transform, that in analyzing a time series signal, can be used to analyze nonlinear and non-stationary signals. The wavelet transform method decomposes a signal into different scale layers with different levels of resolution. The decomposition into different scales is made possible by the fact that the wavelet transform method is based on a square-integrable function and group theory representation. The wavelet transform provides a local representation (both in time and frequency) of a given signal, so it is suitable for analyzing a signal with varying time-frequency resolution, such as the output power of a PV power plant. The mathematical definition for a wavelet transform is as follows.

Let $x(t)$ is a finite energy signal, which satisfies:

$$\int_{-\infty}^{+\infty} |x(t)|^2 dt < \infty \quad (2)$$

The wavelet transform for $x(t)$ is:

$$CWT_{\psi}x(a,b) = W_x(a,b) = \int_{-\infty}^{+\infty} x(t)\psi_{a,b}^*(t)dt \quad (3)$$

where:

$$\psi_{a,b}(t) = |a|^{-\frac{1}{2}} \psi\left(\frac{t-b}{a}\right) \quad (4)$$

$\psi(t)$ is the base function of the mother wavelet, the asterisk denotes the complex conjugate, and a, b are the transform parameters. By the selection of a and b , the wavelet transform provides an elegant algorithm which is known as the WD technique, to decompose a signal into different layers with different time and frequency resolution.

The WD decomposes the given signal $x(n)$ into its detailed smoothed layers. The signal for the power output of a PV power plant contains sharp edges and jumps caused by the fluctuation of the solar radiation, and it has nonlinear characteristics and periodicity. By using the WD method, the output power of the PV power plant is decomposed into two parts; one is the smoothed version of the signal, and the other part contains the detailed version of the signal. Therefore, the WD method discriminates disturbances from the original signal, and can analyze them separately. The idea of the WD is presented in Figure 3.

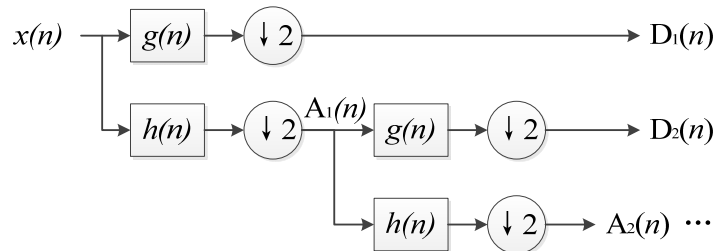


Figure 3. Wavelet decomposition algorithm.

Let $x(n)$ be the discrete-time signal for the output power of a PV power plant. $x(n)$ is to be decomposed into detailed layers and one smoothed layer. From the WD method, the decomposed signals at scale 1 are $A_1(n)$ and $D_1(n)$, where $A_1(n)$ is the smoothed version of the input signal, and $D_1(n)$ is the detailed version of the input signal $x(n)$ in the form of the wavelet transform coefficients. They are defined as:

$$A_1(n) = \sum_k h(k-2n)x(k) \quad (5)$$

$$D_1(n) = \sum_k g(k-2n)x(k) \quad (6)$$

where $h(n)$ and $g(n)$ are the associated filter coefficients that decompose $x(n)$ into $A_1(n)$ and $D_1(n)$. The higher scale decomposition is based on the $A_1(n)$. The decomposed signal at higher scale is given by:

$$A_j(n) = \sum_k h(k-2n)A_{j-1}(k) \quad (7)$$

3.2. Wavelet Decomposition (WD) of Power Signals of a Photovoltaic (PV) Power Plant

WD is conducted for output power signals collected for 5 days from a PV power plant, by a Dmeyer wavelet function with five decomposition layers, shown in Table 3. The decomposition results of the PV power plant output in time-domain signals are shown in Figure 4.

Table 3. Layers Definitions of WD.

Reconstructed Sequence	Definition	Meaning
A5	smoothed signal at 5th layer	reflects change trend of output power of PV power plant, close to theoretically calculated solar irradiance
D5	detailed signal at 5th layer	
D4	detailed signal at 4th layer	
D3	detailed signal at 3rd layer	reflect composition and change rules of high frequency part of signal
D2	detailed signal at 2nd layer	
D1	detailed signal at 1st layer	

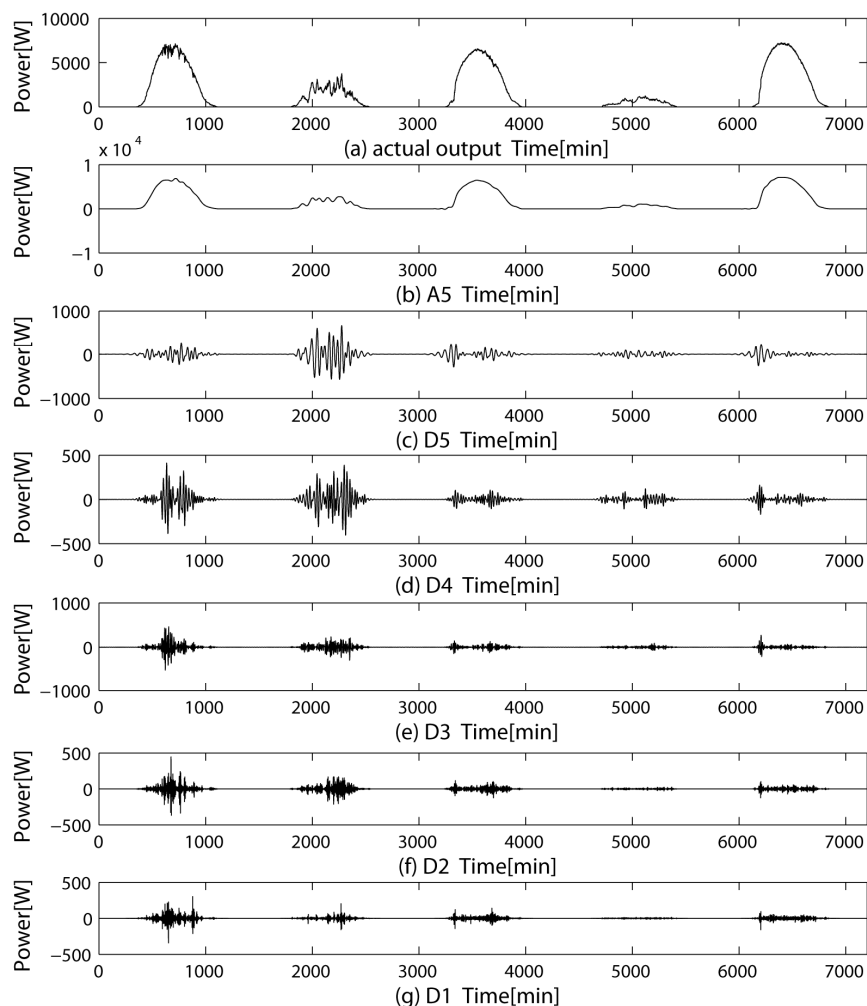


Figure 4. WD of PV output power. (a) Original signal of actual PV output, (b) Smoothed signal of actual PV output at 5th layer, (c) Detailed signal of actual PV output at 5th layer, (d) Detailed signal of actual PV output at 4th layer, (e) Detailed signal of actual PV output at 3rd layer, (f) Detailed signal of actual PV output at 2nd layer, (g) Detailed signal of actual PV output at 1st layer.

It is known from Figure 5 that after 5-layer decomposition layers A5, D5 and D4 can represent the major information of the PV output. Detail signals at other layers represent high-frequency disturbances of meteorological environmental factors on the PV output, which convey less information. Hence, chosen low frequency layers are used in the forecasting model after wavelet decomposition.

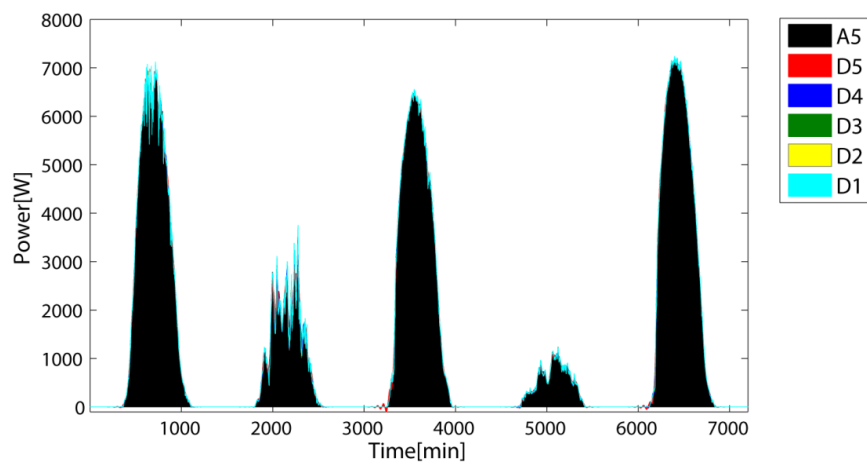


Figure 5. Area graph at each layer.

4. Intelligent Forecasting Model Based on Wavelet Decomposition (WD) and Artificial Neural Network (ANN)

4.1. Artificial Neural Network (ANN) Fundamentals

ANN [6,14–16] is the most popular and widely used tool for artificial intelligence modeling. It is formed by a large numbers of highly related processing elements through an adaptive learning process. ANN has self-adaptiveness, fault tolerance, robustness, and strong inference ability, so it has been successfully applied for power forecasting of wind farms and PV power plant. The ANN is able to learn the complex relationships between the output and the input after training. A basic neural network consists of three layers. They are input layer, hidden layer and output layer as shown in Figure 6.

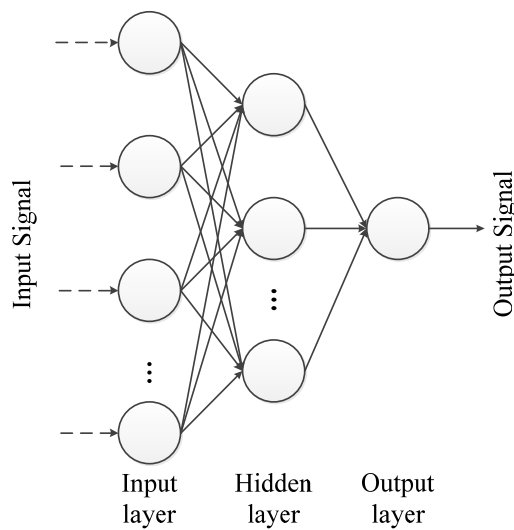


Figure 6. A three-layers artificial neural network.

We use ANN to build the intelligent forecasting model for the output power of the PV power plant. The training of ANN starts with random weights and then neurons works to make sure the error is minimal. The values of the hidden layer neurons is defined by:

$$h_j = f_1(\sum_{i=1}^n v_{ij}x_i + \theta_j) \quad (8)$$

where x_i and h_j are the values of the different layer's neuron; $f_1(\cdot)$ is the sigmoid transfer function; v_{ij} is the adjustable weight between the input and hidden layers and θ_j is the bias of the hidden layer neuron. The hidden layer is the input for the output layer, and the output layer neurons is defined by:

$$o_j = f_2\left(\sum_{i=1}^n w_{ij}h_i + \gamma_j\right) \quad (9)$$

where o_j is the output value of the output layer neuron; $f_2(\cdot)$ is a linear transfer function; w_{ij} is the adjustable weight between the hidden and output layers; γ_j is the bias of the output layer neuron. The three-layer feed-forward neural network is chosen to build the forecasting model in the paper.

4.2. Forecasting Process

Figure 7 shows the working framework for the method presented in the paper. The theoretical solar irradiance [17,18] is the input of the A5 neural network model. Detailed calculation Equations (A1)–(A13) of theoretical solar irradiance are given in Appendix and Figure A1 is the curves of daily theoretical solar irradiance in 15th day of every month.

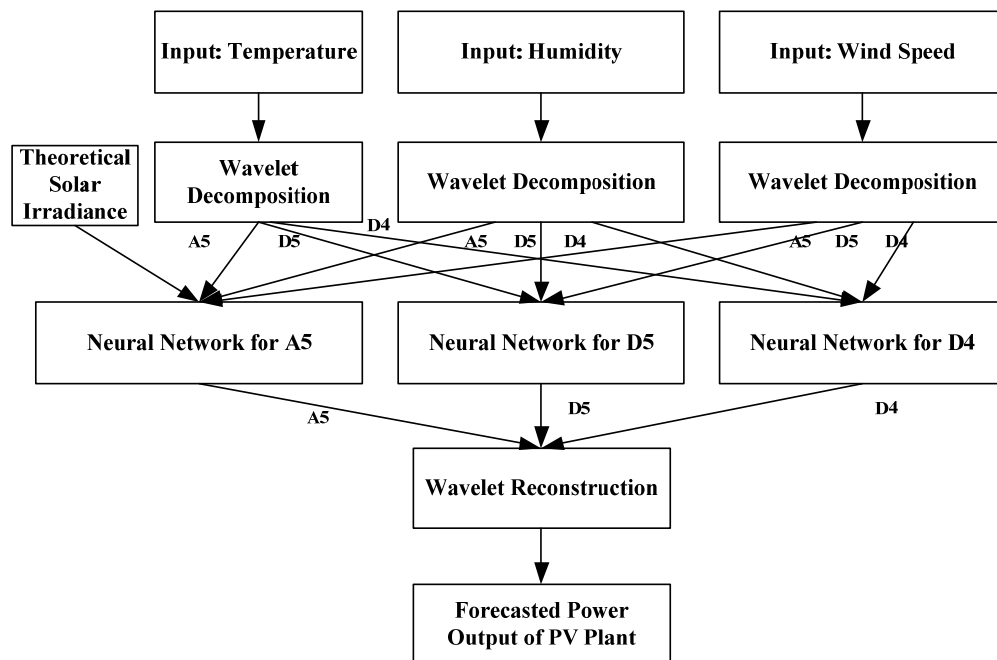


Figure 7. Frame diagram of algorithm.

The forecasting process includes three steps:

Step 1: WD of the output for PV power plant

5-layer WD is carried out for the output power of the PV plant, temperature signal, humidity signal and wind speed signal, followed by the comparison between the approximation layer and detailed layer. Figures 8 and 9 show the smoothed layer A5 and detailed layer D5 after WD. It is known through comparison that the detailed signal part of output power series of PV power plant after multi-scale WD has stationary properties. It is known through Figures 4, 8 and 9 that, through 5-layer WD, the smoothed signal layer can represent the major low frequency information of the original signal. The smoothed signal layers of different signals have good proximity. The periodicity of different signals extracted from the A5 layer is more obvious. Meanwhile, the high frequency interfering noise is filtered well.

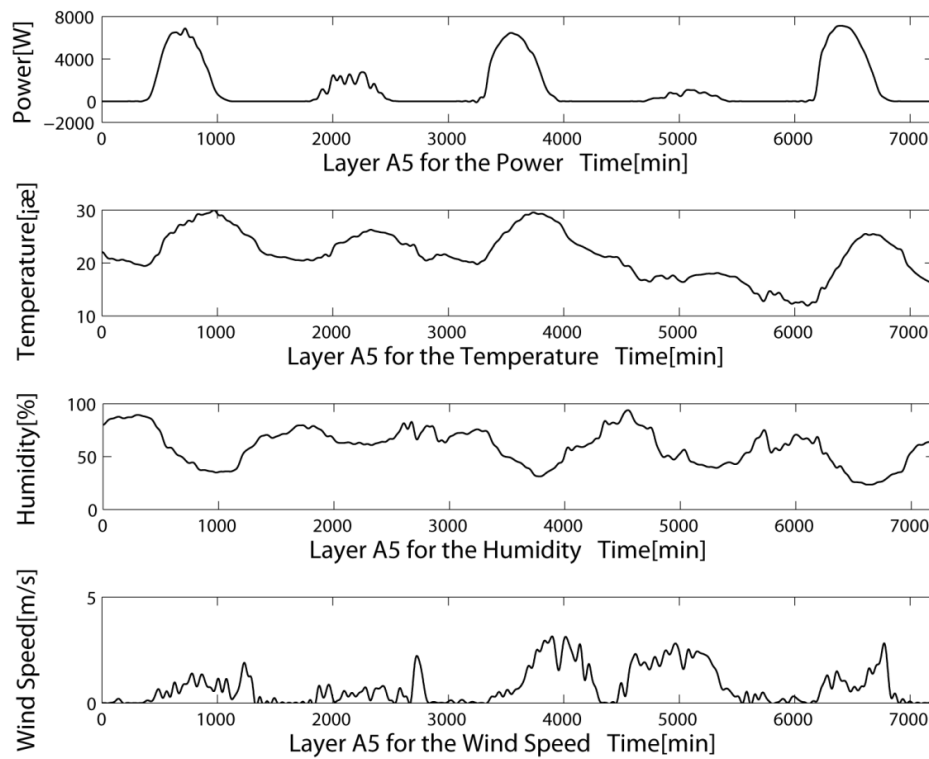


Figure 8. A5 layer comparison of different signals.

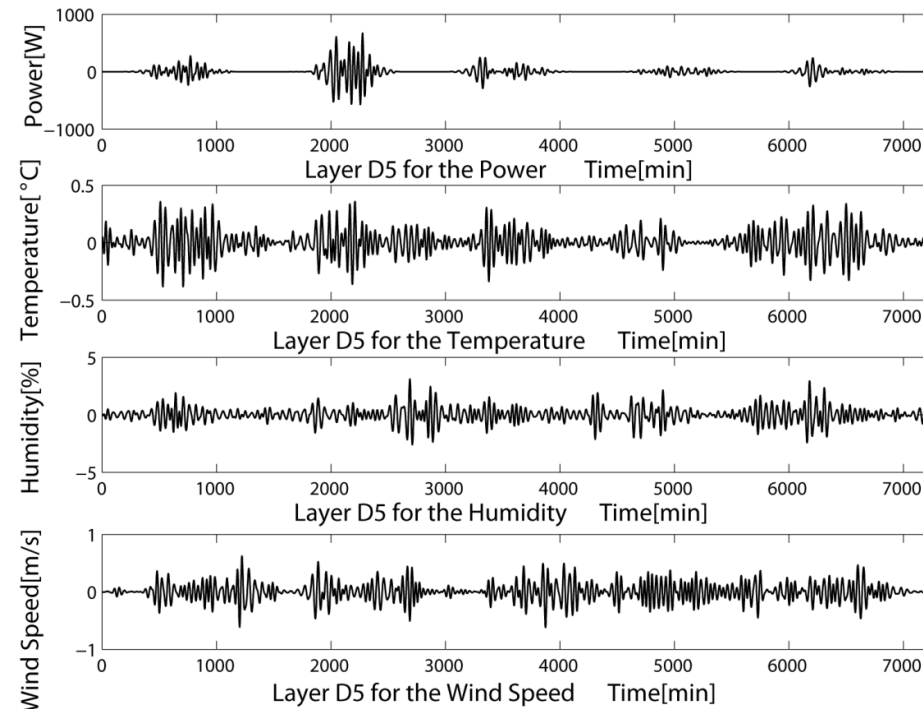


Figure 9. D5 layer comparison of different signals.

Step 2: build ANNs forecasting model

In the physical sense, solar radiation is a direct influencing factor of the voltage effect of PV cells. The irradiance directly influences the output of a photovoltaic cell. Solar irradiance received by a

PV array is influenced by the array installation angle, cloud quantity in the sky and solar position. Meanwhile, the output of a PV power plant is also influenced by meteorological conditions and its own characteristics, but for a known PV power plant, the output time series data of the PV system has a certain autocorrelation. This is because power plant information has been contained in the power output data of the given PV power plant, and complex analysis of the influence of random installation site and operation time on PV system performance degeneration can be avoided. Thus, this paper chooses to use ANNs to establish output power forecasting modeling for PV power plants.

The structure of the forecasting model is shown in Figure 6. An A5 layer neural network is established by selecting A5 smoothed signal layers after WD, including theoretical solar irradiance, temperature, humidity and wind speed signal. The D5 and D4 detailed signal layer after wavelet decomposition of temperature, humidity and wind speed signal are chosen to establish D5 and D4 ANNs. High frequency information at other layers are treated as disturbances for establishing the model, so they are not used.

Step 3: Reconstruction of signals

After different signals are trained for ANNs at each layer, the forecasting results of different signal layers of PV output are obtained. According to Equation (7)—the computational formula of coefficients at different signal layers—signal reconstruction is carried out for the PV power plant power output.

5. Example Analysis and Verification

This paper proposes a hybrid method to forecast the power output of a PV power plant in combination of WD and ANN. To evaluate the effectiveness of this method, it is compared with the forecasting method based on ANN. Figure 10 gives the forecasting performance contrast between the ANN method and WD + ANN method. The solid line shows the measured power output of the PV power plant, while the dotted line shows the output forecast by the two methods. Similarly, the theoretical solar irradiance, temperature, humidity and wind speed are chosen as inputs of the neural network model. The PV power plant power output serves as the target value of the neural network. The WD + ANN method is set up according to Figure 6. It is known from Figure 9 that both the ANN method and WD + AN method can effectively forecast the power output of the PV power plant, but the WD + ANN method can selectively get rid of high-frequency invalid information, and the forecasted power value is closer to the actual measured output.

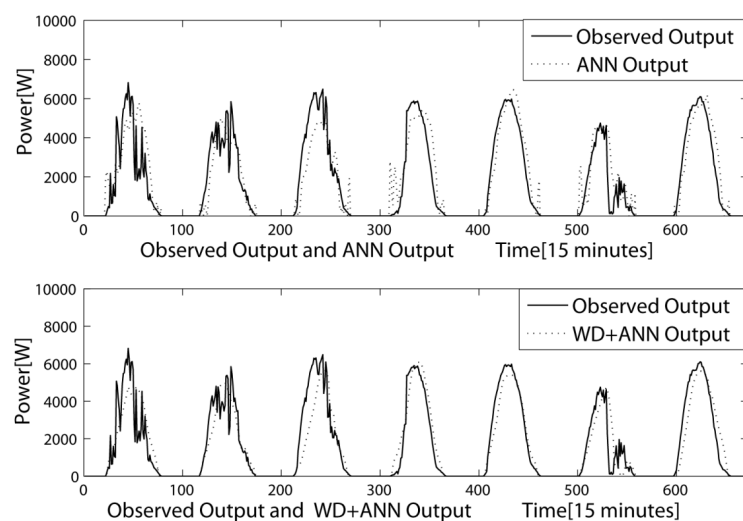


Figure 10. Comparison of forecasted results.

Through comparing forecasting results, on a clear day, WD + ANN has good forecasting precision. On cloudy or rainy days, WD + ANN can reflect different total amounts of output power. However, on cloudy or rainy days, due to abrupt changes in the cloud layer and other environmental factors, the measured power fluctuates greatly, and the forecasting results have a certain deviation. Since it is not possible to effectively forecast the ultra-short term output power variation of the PV power plant on the basis of current weather forecasting technology, it is necessary to consider the application of ground-based observation cloud pictures to correct the forecasting results.

We use root mean square error (RMSE), mean absolute error (MAE) and mean absolute percentage error (MAPE) indexes [1,7] for the assessment of the forecast results based on WD + ANN and ANN. Their definitions are as follows:

$$RMSE = \frac{\sqrt{\sum_{i=1}^n [P_M(i) - P_P(i)]^2}}{Cap \times \sqrt{n}} \times 100\% \quad (10)$$

$$MAE = \frac{\sum_{i=1}^n |P_M(i) - P_P(i)|}{Cap \times n} \times 100\% \quad (11)$$

$$MAPE = \frac{1}{n} \sum_{i=1}^n \left| \frac{P_M(i) - P_f(i)}{P_M(i)} \right| \times 100\% \quad (12)$$

where, $P_M(i)$ is measured power at time i ; $P_f(i)$ is the forecast power at time i ; n is the number of samples; Cap is the mean running capacity.

Calculation of mean running capacity in PV power forecasting is decided by the initial power of the photovoltaic inverter, installed capacity of the PV system and operation time. Factor $Run(i)$ is defined to describe the working state of the PV plant at time i . When the measured power $P_M(i)$ is higher than P_S , the initial power of photovoltaic inverter, then $Run(i)$ equal to 1, meaning that the PV plant is running, else, $Run(i)$ is equal to 0, meaning that the PV plant is not running, as shown in Equation (13):

$$Run(i) = \begin{cases} 1 & , \text{if } P_M(i) > P_S \\ 0 & , \text{if } P_M(i) \leq P_S \end{cases} \quad (13)$$

The definition of Cap is shown in Equation (14):

$$Cap = \frac{\sum_{i=1}^n Run(i)}{n} \times P_r \quad (14)$$

where, P_S is initial power of the photovoltaic inverter; P_r is installed capacity of the PV system. Equations (13) and (14) can eliminate the accumulated calculation during nighttime when the PV plant stops working.

Table 4 shows the assessment results of different methods to better understand the effect of using WD + ANN and ANN under various different weather conditions. It is known from Table 4 that the WD + ANN method has better forecasting precision and convergence speed than the ANN method under different weather conditions.

Table 4. Comparison of forecasting performance between ANN and WD + ANN model on clear, cloudy, overcast, rainy days.

Model	Weather	Error			Convergence Epochs
		RMSE(%)	MAE(%)	MAPE(%)	
ANN	clear	9.313	4.978	13.858	4521
	cloudy	18.472	10.259	21.550	
	overcast	18.511	10.220	35.226	
	rainy	22.948	13.062	30.926	
WD + ANN	clear	7.193	3.639	9.240	2677
	cloudy	16.817	9.578	21.294	
	overcast	17.607	10.544	26.767	
	rainy	19.663	10.349	25.373	

6. Conclusions

This paper puts forward a method to forecast the power output of PV power plants based on WD and ANN. Due to the periodic and non-stationary characteristics of the power output series of a PV power plant, the wavelet analysis method is adopted to carry out multi-scale decomposition of the PV output. A smoothed signal and detailed signal of the PV output are obtained. Forecasting models at different signal layers are established through ANN. Finally, through construction of the forecasting results of different signal layers, the forecasting results of the PV power plant are obtained. Through comparison to the ANN method, it is shown that the forecasting method proposed in this paper has better forecasting precision, and less algorithm convergence time.

Acknowledgments: The authors would like to acknowledge the financial support of the Beijing Higher Education Young Elite Teacher Project (YETP0714), the Program of the Co-Construction with Beijing Municipal Commission of Education, State Key Laboratory of Alternate Electrical Power System with Renewable Energy Sources (LAPS14006).

Author Contributions: All authors contributed to this work by collaboration. Honglu Zhu is the first author in this manuscript. All authors revised and approved for the publication.

Conflicts of Interest: The authors declare no conflict of interest.

Appendix

This Appendix gives details on the equation for calculating the theoretical solar irradiance (Figure 6):

$$E_g = E_{dir} + E_{dif} \quad (A1)$$

where, E_g is the global horizontal irradiance; E_{dir} is the direct horizontal irradiance; E_{dif} is the diffuse horizontal irradiance. The direct and diffuse horizontal irradiance can be calculated according to the following steps [15,16]: according to the Cooper formula, the declination angle is calculated by the following equation:

$$\delta = 23.45 \times \sin(360^\circ \times \frac{284 + n}{365}) \quad (A2)$$

where, n is the ordinal number of the date.

Calculation of the solar hour angle starts from 0° at 12:00 am, and every hour represents 15° . For instance, 14:00 pm and 10:00 am represent 30° and -30° . The azimuth angle takes south direction as 0° , and west as positive. We account for the influence of the time difference on hour angle, since the longitude of Beijing is 120° E, so the computational equation of hour angle ω in China is:

$$\omega = (12 - t) \times 15^\circ + (120^\circ - \Psi) \quad (A3)$$

where, t is the Beijing time; Ψ is the longitude.

Calculation of the solar altitude angle can be conducted as follows:

$$\sin h = \sin \phi \times \sin \delta + \cos \phi \times \cos \delta \times \cos \omega \quad (A4)$$

where, ϕ is the latitude.

The computational formula of the extraterrestrial normal irradiance is:

$$E_0 = E_{SC} \times [1 + 0.034 \times \cos\left(\frac{2\pi n}{365}\right)] \quad (\text{A5})$$

where, E_{SC} is solar constant, equal to 1367 W/m^2 .

The degree of influence of the atmosphere on sunlight received by the Earth surface is defined as air mass (AM). Air mass is a dimensionless quantity. It is the ratio of the path of solar rays passing through the atmosphere and the path of solar rays passing through the atmosphere in the zenith angle direction. Assuming that standard atmospheric pressure is $101,325 \text{ Pa}$ and air temperature is 0°C , the vertical incidence path of solar rays at sea level is defined as 1. According to the value of the solar altitude angle h , air mass m should be calculated in two situations. When $h \geq 30^\circ$, air mass m is:

$$m(h) = 1/\sin h \quad (\text{A6})$$

when $h < 30^\circ$:

$$m(h) = [1229 + (614 \times \sin h)^2]^{1/2} - 614 \times \sin h \quad (\text{A7})$$

Generally, the influence of temperature on m is neglected, but in high altitude regions, the atmospheric pressure should be corrected, *i.e.*,

$$m(z, h) = m(h) \frac{P(z)}{P_0} \quad (\text{A8})$$

$$P(z)/P_0 = [(288 - 0.0065 \times z)/288]^{5.256} \quad (\text{A9})$$

where, z is the elevation.

The atmospheric transparency coefficient is used to represent the degree of attenuation of the solar radiation by the atmosphere. On a clear day, the solar direct radiation is influenced by air mass. Meanwhile, molecular scattering, ozone absorption and selective absorption of some gases ($\text{CO}_2, \text{O}_2, \text{N}_2$) influence the penetrability of solar radiation. Hence, the atmospheric transparency coefficient is related to local atmospheric conditions:

$$\tau_{dir} = 0.56 \times (e^{-0.56m(z,h)} + e^{-0.096m(z,h)}) \quad (\text{A10})$$

The atmospheric transparency coefficient of diffuse irradiance is:

$$\tau_{dif} = 0.2710 - 0.2939 \times \tau_{dir} \quad (\text{A11})$$

On a clear day, the direct solar radiation accounts for the main part of global solar radiation. In view of the atmospheric attenuation and solar altitude, direct horizontal irradiance at any time can be figured out as follows:

$$E_{dir} = E_0 \times \tau_{dir} \times \sin h \times k_1 \quad (\text{A12})$$

where, k_1 is an empirical coefficient of atmospheric turbidity. In direct solar radiation calculations, it ranges from 0.8 to 0.9.

Diffuse horizontal radiation is complex. It is related to scattering distribution (cloud shape, cloud quantity and atmosphere). Diffuse irradiance arriving at horizontal level is E_{dif} , and the calculation formula is as follows:

$$E_{dif} = \frac{1}{2} \times E_0 \times \sin h \times \frac{1 - \tau_{dif}}{1 - 1.4 \ln[\tau_{dif}/m(z, h)]} \times k_2 \quad (\text{A13})$$

where, k_2 is an empirical coefficient of atmospheric turbidity. In diffuse solar radiation calculations, it ranges from 0.60 to 0.90. When the atmosphere is turbid, $0.60 \leq k_2 \leq 0.70$. When it is normal, $0.710 \leq k_2 \leq 0.80$. When it is good, $0.810 \leq k_2 \leq 0.90$.

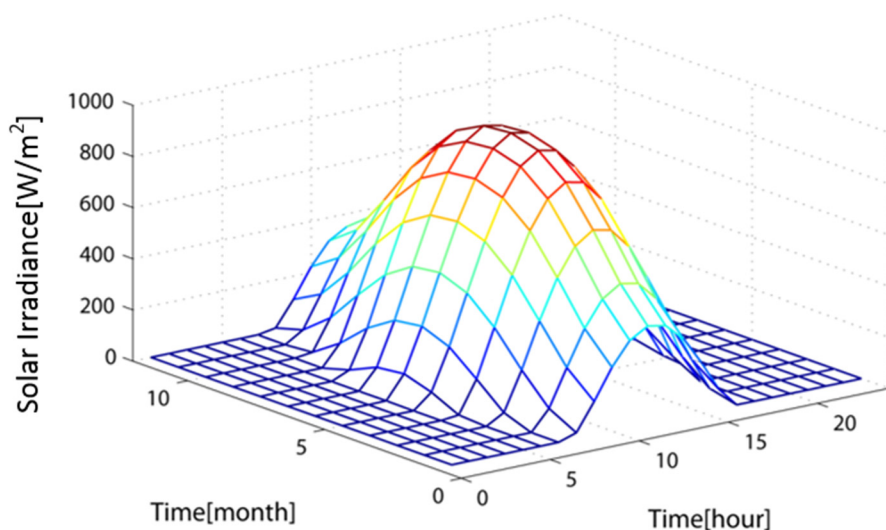


Figure A1. Theoretical solar irradiance.

References

- Mandal, P.; Madhira, S.T.S.; haque, A.U.; Meng, J.; Pineda, R.L. Forecasting power output of solar photovoltaic system using wavelet transform and artificial intelligence techniques. *Procedia Comput. Sci.* **2012**, *12*, 332–337. [[CrossRef](#)]
- Ogliari, E.; Grimaccia, F.; Leva, S.; Mussetta, M. Hybrid predictive models for accurate forecasting in PV systems. *Energies* **2013**, *6*, 1918–1929. [[CrossRef](#)]
- Lorenz, E.; Scheidsteiger, T.; Hurka, J.; Heinemann, D.; Kurz, C. Regional PV power prediction for improved grid integration. *Prog. Photovolt.* **2010**, *19*, 757–771. [[CrossRef](#)]
- Lorenz, E.; Heinemann, D.; Kurz, C. Local and regional photovoltaic power prediction for large scale grid integration: Assessment of a new algorithm for snow detection. *Prog. Photovolt.: Res. Appl.* **2012**, *20*, 760–769. [[CrossRef](#)]
- Karthikeyan, L.; Nagesh Kumar, D. Predictability of nonstationary time series using wavelet and EMD based ARMA models. *J. Hydrol.* **2013**, *502*, 103–119. [[CrossRef](#)]
- Mellit, A.; Kalogirou, S.A. Artificial intelligence techniques for photovoltaic applications: A review. *Prog. Energy Combust. Sci.* **2008**, *34*, 574–632. [[CrossRef](#)]
- Pedro, H.T.C.; Coimbra, C.F.M. Assessment of forecasting techniques for solar power production with no exogenous inputs. *Sol. Energy* **2012**, *86*, 2017–2028. [[CrossRef](#)]
- Voyant, C.; Muselli, M.; Paoli, C.; Nivet, M.-L. Numerical weather prediction (NWP) and hybrid ARMA/ANN model to predict global radiation. *Energy* **2012**, *39*, 341–355. [[CrossRef](#)]
- Monteiro, C.; Santos, T.; Fernandez-Jimenez, L.; Ramirez-Rosado, I.; Terreros-Olarte, M. Short-term power forecasting model for photovoltaic plants based on historical similarity. *Energies* **2013**, *6*, 2624–2643. [[CrossRef](#)]
- Mellit, A.; Benghanem, M.; Kalogirou, S.A. An adaptive wavelet-network model for forecasting daily total solar-radiation. *Appl. Energy* **2006**, *83*, 705–722. [[CrossRef](#)]
- Fryzlewicz, P.; van Bellegem, S.; von Sachs, R. Forecasting non-stationary time series by wavelet process modelling. *Ann. Inst. Stat. Math.* **2003**, *55*, 737–764. [[CrossRef](#)]
- Catalão, J.P.S.; Pousinho, H.M.I.; Mendes, V.M.F. Short-term wind power forecasting in Portugal by neural networks and wavelet transform. *Renew. Energy* **2011**, *36*, 1245–1251. [[CrossRef](#)]
- Domingues, M.O.; Mendes, O.; da Costa, A.M. On wavelet techniques in atmospheric sciences. *Adv. Space Res.* **2005**, *35*, 831–842. [[CrossRef](#)]
- Mellit, A.; Pavan, A.M. A 24-h forecast of solar irradiance using artificial neural network: Application for performance prediction of a grid-connected PV plant at Trieste, Italy. *Sol. Energy* **2010**, *84*, 807–821. [[CrossRef](#)]

15. Azadeh, A.; Maghsoudi, A.; Sohrabkhani, S. An integrated artificial neural networks approach for predicting global radiation. *Energy Convers. Manag.* **2009**, *50*, 1497–1505. [[CrossRef](#)]
16. Chen, S.H.; Jakeman, A.J.; Norton, J.P. Artificial intelligence techniques: An introduction to their use for modelling environmental systems. *Math. Comput. Simul.* **2008**, *78*, 379–400. [[CrossRef](#)]
17. Kumar, L.; Skidmore, A.K.; Knowles, E. Modelling topographic variation in solar radiation in a GIS environment. *Int. J. Geogr. Inf. Sci.* **1997**, *11*, 475–497. [[CrossRef](#)]
18. Gueymard, C.A. Clear-sky irradiance predictions for solar resource mapping and large-scale applications: Improved validation methodology and detailed performance analysis of 18 broadband radiative models. *Sol. Energy* **2012**, *86*, 2145–2169. [[CrossRef](#)]



© 2015 by the authors; licensee MDPI, Basel, Switzerland. This article is an open access article distributed under the terms and conditions of the Creative Commons by Attribution (CC-BY) license (<http://creativecommons.org/licenses/by/4.0/>).